Available online at website: https://journal.bcrec.id/index.php/jcerp

Journal of Chemical Engineering Research Progress, 3 (2) 2026, 350-360

Original Research Article

Response Surface Optimization of Setting Time and Compressive Strength of a Clay–Bauxite Geopolymer Binder for Oil-Well Cementing

Barima Money[1], Priyanga A/P Kailasanathan[2], Norasyikin Ismail[1], Abutu David[1], Siti Hajar Noor Shaarani[1], Norida Ridzuan[1], Siti Qurratu' Aini Mahat[1*]

[1]*Faculty of Chemical and Process Engineering Technology, Universiti Malaysia Pahang, Al-Sultan Abdullah, Lebuhraya Persiaran Tun Khalil Yaakob 26300 Kuantan, Pahang, Malaysia.*

[2]*Faculty of Medicine, Widad University College, BIM Point, Bandar Indera Mahkota, 25200 Kuantan, Pahang, Malaysia.*

Received: 18th May 2026; Revised: 1st August 2026; Accepted: 3rd August 2026
Available online: 5th August 2026; Published regularly: December 2026

Abstract

The development of sustainable cement alternatives has intensified interest in alkali-activated binders formulated from abundant clay minerals. In this study, a clay-based geopolymer binder was synthesized and optimized by investigating the combined influence of activated clay loading (10-100 g), bauxite loading (0-150 g), alkaline activator dosage (0-3 g), and curing temperature (90-150 °C) on its setting time and compressive strength. A Central Composite Design (CCD) under Response Surface Methodology (RSM) was employed to model the responses and determine optimal processing conditions. The experimental results revealed that both responses were significantly influenced by the synergy between the activator dosage and raw material loading. Increasing activated clay and bauxite content accelerated geopolymerization, leading to shortened setting time, whereas excessive activator addition resulted in delayed matrix hardening due to excess soluble silicate–aluminate species. Compressive strength increased with increasing precursor loading up to a threshold level, beyond which incomplete dissolution restricted polycondensation. Regression analysis demonstrated excellent agreement between predicted and experimental values, with no transformation required, as confirmed by Box–Cox analysis. The normality and independence of residuals were verified through residual plots against predicted values and experimental runs. Optimization using a desirability function achieved a setting time of 6 h and compressive strength of 40.44 MPa at optimal conditions of activated clay (55 g), bauxite (75 g), activator dosage (1.5 g), and curing temperature (120 °C), with a global desirability of 1.000. These results confirm RSM as an effective statistical tool for tailoring the performance of clay-based geopolymers, offering a promising pathway for developing high-strength, fast-setting, sustainable binders.

Keywords: Clay-based geopolymer; Response Surface Methodology (RSM); Setting time optimization; Compressive strength; Central Composite Design (CCD)

How to Cite: Money, B., Kailasanathan, P. A., Ismail, N., David, A., Shaarani, S. H. N., Ridzuan, N., Aini Mahat, S. Q. (2026). Response Surface Optimization of Setting Time and Compressive Strength of a Clay–Bauxite Geopolymer Binder for Oil-Well Cementing. *Journal of Chemical Engineering Research Progress*, 3 (2), 350-360 (DOI: 10.9767/jcerp.20745)

Permalink/DOI: https://doi.org/10.9767/jcerp.20745

1. Introduction

Oil-well cementing plays a vital role in drilling and well completion. It ensures zonal isolation, supports the casing, and maintains long-term wellbore stability [1-3]. To perform effectively, the cement must withstand extreme downhole conditions such as high temperatures, high pressures, corrosive fluids, and repeated stress cycles. Because of this, the American Petroleum Institute (API) sets strict requirements for properties like setting time, compressive strength, rheology, and durability [4-6]. Ordinary Portland cement (OPC) has long been the standard material for oil-well cementing.

* Corresponding Author.
Email: sitiqurratu@umpsa.edu.my (S.Q.A. Mahat).

However, its performance can decline under harsh downhole conditions. At high temperatures, its hydration products begin to degrade, leading to a loss of strength, increased permeability, and potential failure of zonal isolation [7]. OPC is also vulnerable to chemical attacks from sulfates, CO_2, and aggressive formation fluids. Beyond technical limitations, OPC production is energy-intensive and contributes significantly to global CO_2 emissions, increasing the demand for more sustainable alternatives [8-10].

Geopolymer cement has emerged as a promising substitute. Produced through the alkaline activation of aluminosilicate materials, geopolymers offer high strength, faster setting, improved thermal stability, and strong resistance to chemical attack [11-13]. Their low calcium content enhances performance at elevated temperatures, making them better suited for deep and high-temperature wells. In addition, geopolymer production generates considerably lower CO_2 emissions compared to OPC. Among these alternatives, clay-based geopolymers (CBG), especially those derived from calcined clays, are particularly attractive due to their abundance, affordability, and consistent composition. When combined with materials such as bauxite or agricultural ashes, they can be engineered to meet the strength and durability requirements of oil-well applications [9,13,14]. However, their performance depends on several interacting factors, including precursor content, activator concentration, and curing temperature. Traditional trial-and-error methods are insufficient to understand these interactions fully. Response Surface Methodology (RSM) offers a systematic and efficient way to model these variables and determine optimal conditions. While widely used in materials research, it has been less explored for CBG designed specifically for oil-well cementing [15,16].

Despite these advancements, significant research gaps remain [17]. Most previous studies have focused on evaluating geopolymer formulations using conventional experimental approaches that investigate individual factors independently, thereby providing limited understanding of the interactive effects among clay loading, bauxite content, alkaline activator concentration, and curing temperature. Moreover, although Response Surface Methodology (RSM) has been successfully applied in various materials optimization studies, its application to clay-based geopolymer systems specifically developed for oil-well cementing remains limited [18,19]. Consequently, there is still a lack of statistically validated predictive models capable of optimizing multiple formulation variables simultaneously to satisfy the stringent performance requirements of oil-well cement. The novelty of this study lies in the development of an optimized clay–bauxite geopolymer cement specifically designed for oil-well applications through the integration of RSM-based modelling and optimization [19]. In addition to identifying the optimum formulation, this study establishes predictive mathematical models that quantify the interactions between critical processing variables and their influence on setting time and compressive strength [20]. These findings provide new scientific knowledge for designing high-performance, low-carbon geopolymer cement systems suitable for harsh downhole environments and offer a practical optimization framework that extends beyond previous studies.

This study, therefore, aims to optimize CBG cement for oil-well applications using RSM. It investigates the effects of clay loading, bauxite content, activator concentration, and curing temperature on setting time and compressive strength, develops predictive models, and identifies the optimal formulation suitable for downhole conditions. Through this approach, the research contributes to the development of high-performance, low-carbon alternatives to conventional oil-well cement.

2. Materials and Methods

The selection of the experimental variables was based on their well-established influence on the geopolymerization process and the engineering performance of geopolymer binders reported in previous studies [19-21]. Activated clay loading, bauxite loading, alkaline activator loading, and curing temperature were therefore selected as the independent variables because they directly control the dissolution of aluminosilicate species, geopolymer gel formation, reaction kinetics, and microstructural development of the geopolymer matrix. Variations in activated clay and bauxite loadings determine the availability and balance of reactive silica and alumina necessary for geopolymer network formation, while the alkaline activator loading governs the extent of precursor dissolution and polymerization [21]. Likewise, curing temperature significantly affects the rate of geopolymerization and the degree of matrix densification. These factors collectively influence the final engineering properties of the geopolymer [22]. Consequently, compressive strength and setting time were selected as the dependent variables because they represent the primary performance indicators for evaluating the suitability of geopolymer cement in oil-well cementing applications. Compressive strength reflects the load-bearing capacity and structural integrity of the hardened cement, whereas setting time determines its placement characteristics and operational feasibility during well cementing [22,23]. Therefore, the dependent variables are direct responses to changes in the selected independent variables, making them appropriate response parameters for optimization using RSM.

2.1 Materials and Clay Precursor

The primary aluminosilicate precursor used in this study was natural clay collected from the Kuala Rompin region in Pahang, Malaysia. Kuala Rompin Clay (KRC) is geologically associated with tropical residual soil formations, predominantly composed of kaolinite with minor quantities of quartz, hematite, and feldspar. The clay deposit is characterized by fine-grained particles formed through prolonged weathering of silicate-rich parent rock, making it suitable for geopolymer synthesis due to its high alumina and silica content and structural reactivity upon calcination.

2.2. Pre-Treatment of Raw Clay

The primary aluminosilicate precursor used in this study was natural clay collected from the Kuala Rompin region in Pahang, Malaysia. KRC is geologically associated with tropical residual soil formations, predominantly composed of kaolinite with minor quantities of quartz, hematite, and feldspar. The clay deposit is characterized by fine-grained particles formed through prolonged weathering of silicate-rich parent rock, making it suitable for geopolymer synthesis due to its high alumina and silica content and structural reactivity upon calcination.

2.3. Calcination Procedures

To transform the raw clay into a reactive metakaolinized precursor, controlled thermal activation was performed using a muffle furnace. The clay powder was heated at a rate of 10 °C/min to a peak temperature of 1200 °C and maintained for 2 hours [22]. This temperature range was selected based on dehydroxylation thresholds for kaolinitic clays, ensuring the breakdown of structural hydroxyl groups while avoiding the formation of spinel or mullite phases that reduce reactivity. The calcined material (metakaolinized KRC) was then cooled in a desiccator to prevent moisture uptake.

2.4. Preparation and Aging

The NaOH solution was prepared 24 hours before mixing to ensure complete dissolution and thermal stabilization. It was then combined with the sodium silicate solution at predetermined ratios based on the RSM design. The activator mixture was allowed to equilibrate at room temperature for at least one hour before geopolymer synthesis to ensure consistent viscosity and chemical activity. Bauxite and Empty Fruit Bunch Ash (EFBA) were used as supplementary aluminosilicate sources in the geopolymer formulation. Bauxite, rich in Al_2O_3 (over 45% as confirmed by XRF; see Table 1), provided additional alumina to enhance network formation, while EFBA, an agricultural by-product from the palm oil industry, supplied amorphous silica, as evidenced by XRD analysis. Their inclusion served to optimize the silica–alumina ratio, improve geopolymer gel formation and mechanical strength, enhance thermal stability for oil-well applications, and promote sustainability through the use of locally available waste materials.

2.5. Design of Experimental

2.5.1. Response Surface Methodology (RSM) framework

RSM was employed to evaluate the effects of multiple interacting factors on the performance of CBG and to determine the optimum conditions for oil-well cementing applications [22,23]. A Box–Behnken Design (BBD) was adopted due to its efficiency, reduced number of experimental trials, and suitability for quadratic surface modeling, without requiring extreme (high or low) factor-level combinations, as seen in Table 2. BBD is particularly advantageous for materials research where extreme values of factors, such as excessively high alkali concentration or temperature, may lead to impractical or unsafe conditions that distort true material behavior. Alternatively, Central Composite Design (CCD) is commonly used in optimization studies; however, CCD generally requires more factorial points and includes axial points that may fall outside the practical ranges of geopolymer processing

Table 1. XRF results showing the chemical composition of KRC, EFBA, and Bauxite by wt%.

Oxide (%)	SiO_2	Al_2O_3	Fe_2O_3	CaO	MgO	Na_2O	K_2O	SO_3	TiO_2	P_2O_5
KRC	23.1	40.8	1.71	2.02	2.08	2.21	2.22	1.06	1.22	1.01
EFBA	20.1	1.70	2.12	0.9	1.20	2.05	43.9	1.45	1.84	-
Bauxite	6.21	21.3	1.16	2.76	1.80	-	3.15	-	0.78	-

variables. Since the goal of this study was to capture curvature effects while maintaining experimental feasibility, BBD was selected as the optimal design strategy [22-24]. The RSM framework enabled the development of predictive regression equations, analysis of factor significance using analysis of variance (ANOVA), and generation of contour and response surface plots to visualize interactions among key process variables.

3. Results and Discussion

The mechanical and rheological performance of the CBG cement was strongly influenced by the interplay among precursor composition, alkaline activator concentration, and curing temperature. The RSM-based experimental design produced compressive strengths ranging from 31.5 to 48.8 MPa and setting times between 2 and 8 hours, demonstrating a wide variability that reflects the sensitivity of the geopolymer system to changes in mix parameters. Importantly, many formulations surpassed the API-recommended compressive strength for oil-well cementing (35 MPa), illustrating the viability of clay-based geopolymers for high-temperature downhole applications.

3.1. Analysis and Discussion of the Contour Plot of Compressive Strength as Influenced by Activated Clay Loading (A) and Temperature (D).

The RSM results in Figure 1 (a–d) clearly show that compressive strength optimization is controlled by the combined effects of activated clay loading (A), bauxite loading (B), alkaline activator loading (C), and curing temperature (D). Figure 1 (a) indicates that compressive strength increases markedly with increasing alkaline activator loading, confirming that C is the most influential parameter due to its role in enhancing aluminosilicate dissolution and geopolymer gel formation [24-25]. High bauxite content alone is insufficient at low activator levels, highlighting the need for adequate activation of solid precursors. Figure 1 (b) shows that simultaneous increases in activated clay and bauxite lead to a steady, near-linear increase in strength at constant activator dosage and temperature.

Table 2. Illustration of all the factors, responses of compressive strength, and setting time.

Std	Run	Factor 1	Factor 2	Factor 3	Factor 4	Response 1	Response 2
		Activated Clay Loading	Bauxite Loading	Alkaline Activator Loading	Temperature	Compressive strength	Setting time
		g	g	g	°C	Mpa	Hour
11	1	10	75	1.5	150	39.7	5.00
1	2	10	0	1.5	120	33.5	8.00
22	3	55	150	1.5	90	39.8	6.00
24	4	55	150	1.5	150	45.5	3.00
13	5	55	0	0	120	32.0	8.00
20	6	100	75	3	120	48.8	3.00
23	7	55	0	1.5	150	40.6	5.00
18	8	100	75	0	120	38.6	6.00
29	9	55	75	1.5	120	40.0	6.00
28	10	55	75	1.5	120	40.2	6.00
15	11	55	0	3	120	42.8	5.00
3	12	10	150	1.5	120	39.0	6.00
10	13	100	75	1.5	90	40.6	6.00
6	14	55	75	3	90	42.5	5.00
2	15	100	0	1.5	120	41.2	6.00
5	16	55	75	0	90	31.5	8.00
14	17	55	150	0	120	38.8	6.00
17	18	10	75	0	120	32.0	8.00
19	19	10	75	3	120	41.6	5.00
27	20	55	75	1.5	120	40.8	6.00
12	21	100	75	1.5	150	46.6	3.00
9	22	10	75	1.5	90	36.5	7.00
21	23	55	0	1.5	90	34.8	8.00
25	24	55	75	1.5	120	40.4	6.00
8	25	55	75	3	150	47.9	2.00
7	26	55	75	0	150	37.2	5.00
4	27	100	150	1.5	120	46.9	4.00
16	28	55	150	3	120	48.2	3.00
26	29	55	75	1.5	120	40.8	6.00

Activated clay provides the primary reactive silica–alumina framework, while bauxite supplies additional alumina to optimize the Al/Si ratio. Figure 1(c) further confirms the dominance of alkaline activator loading, as strength increases more sharply along the activator axis than along the clay axis, indicating that sufficient activator is required to realize the reactive potential of activated clay fully [25]. Figure 1 (d) demonstrates that a higher curing temperature, combined with an increased activated clay content, enhances compressive strength by accelerating geopolymerization kinetics and matrix densification. The optimum compressive strength is achieved at high alkaline activator loading, high activated clay content, moderate-to-high bauxite loading, and elevated curing temperature. These results confirm that all parameters contribute to strength development, with activator loading as the key controlling factor, supporting the research objective of producing a high-strength geopolymer suitable for oil-well cementing applications [25,26].

3.2. Analysis and Discussion of the Predicted vs. Actual Plot for Compressive Strength.

Figure 2 (a–d) presents the optimization and validation results for compressive strength using RSM. Figure 2 (a) shows the 3D surface plot of alkaline activator loading (*C*) and curing temperature (*D*) at fixed activated clay (A = 55 g) and bauxite loading (B = 75 g). Compressive strength increases with both higher activator dosage and elevated curing temperature, confirming their combined role in enhancing aluminosilicate dissolution, reaction kinetics, and geopolymer gel development [27,28]. Figure 2 (b) compares predicted and experimental compressive strength values. The close clustering of data points along the 45° reference line indicates excellent agreement between predicted and actual responses, confirming the robustness and predictive accuracy of the developed model. Figure 2 (c) presents the numerical optimization results based on the desirability function. The optimal conditions were identified as activated clay loading of 55 g, bauxite loading of 75 g, alkaline activator loading of 1.5 g, and curing

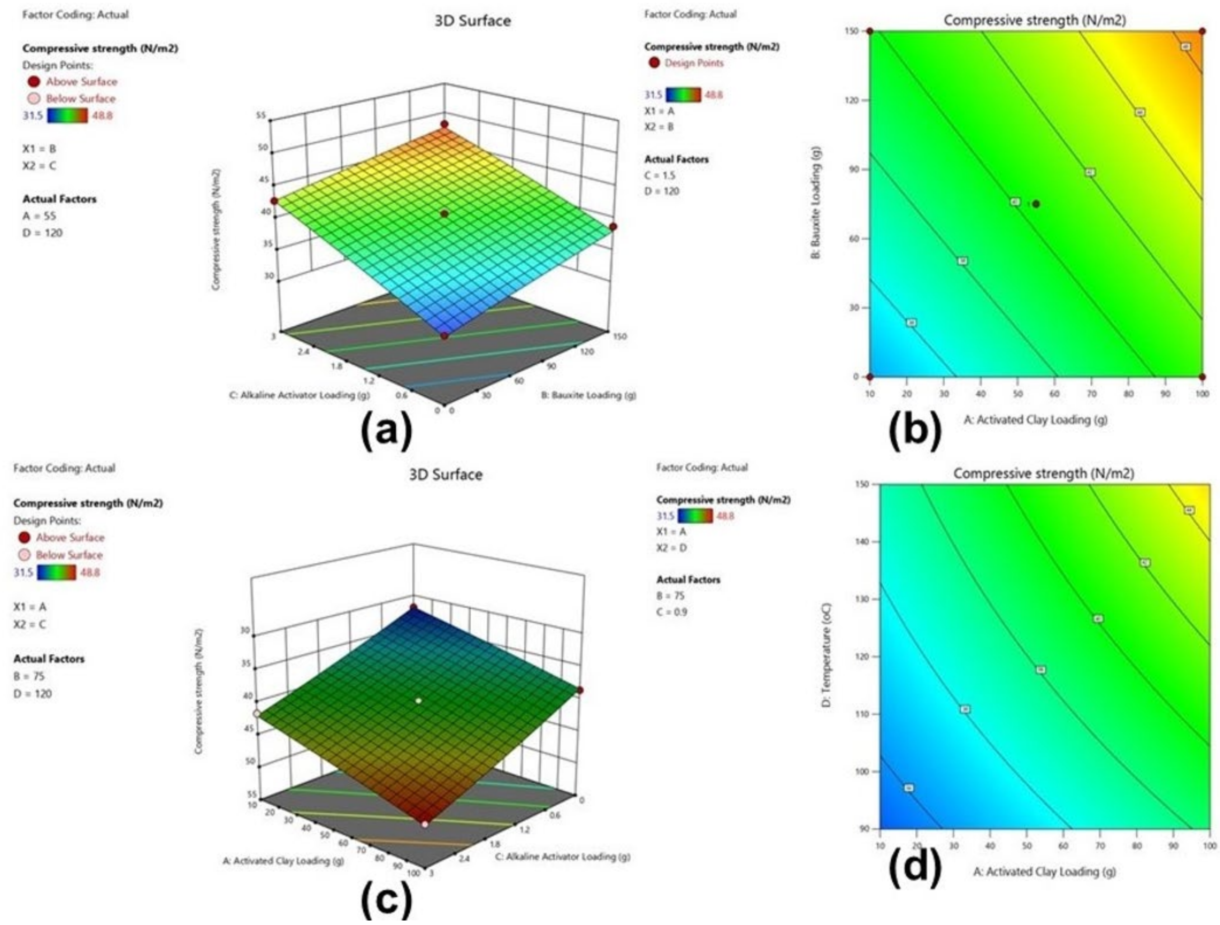

Figure 1. Response surface and contour plots illustrate the effects of activated clay, bauxite, alkaline activator, and curing temperature on compressive strength optimization.

temperature of 120 °C, yielding a predicted compressive strength of approximately 40.4 MPa with a desirability value of 1.0. This confirms that the selected factor combination satisfies the optimization criteria. Figure 2 (d) shows the overlay plot, where the highlighted region represents the feasible design space meeting the target compressive strength requirements [28,29]. The location of the optimal point within this region demonstrates a stable and well-defined operating window. These results confirm that compressive strength optimization is primarily controlled by alkaline activator loading and curing temperature, with activated clay and bauxite providing the necessary reactive framework. The strong agreement between model predictions and experimental data validates the suitability of the optimized mix design for oil-well cementing applications. The empirical mathematical model for compressive strength is as follow:

$$Y_{cs} = +39.04 - 0.0750A - 1.93B - 0.1500C - 0.3417D + 2.29AB + 0.0125AC + 0.7250AD - 0.4125BC + 0.9750BD + 0.9500CD + 0.8004A^2 + 1.23B^2 + 0.1379C^2 - 0.6371D^2 \quad (1)$$

where A is activated clay loading (g), B is bauxite loading (g), C is alkaline activator loading (g), D is curing temperature (°C), and Y_{cs} is predicted compressive strength (MPa).

3.3. Analysis and Discussion of the Contour Plot of Setting Time as Influenced by Activated Clay Loading (*A*) and Temperature (*D*)

Figure 3 (a–d) presents the response surface and contour plot analyses for setting time optimization of the geopolymer system. Figure 3 (a) illustrates the combined influence of activated clay loading (*A*) and bauxite loading (*B*) on setting time at fixed alkaline activator loading (C = 1.5 g) and curing temperature (D = 120 °C). Setting time increases gradually with increasing contents of both solid precursors, indicating that higher solid loadings slow down the setting process due to increased solid–liquid interactions and reduced effective activator availability [30,31]. The corresponding contour plot in Figure 3 (b) confirms this trend, showing longer setting times at higher levels of activated clay and bauxite. The smooth and nearly parallel contour lines indicate a predominantly linear response, suggesting limited interaction between *A* and *B* within the

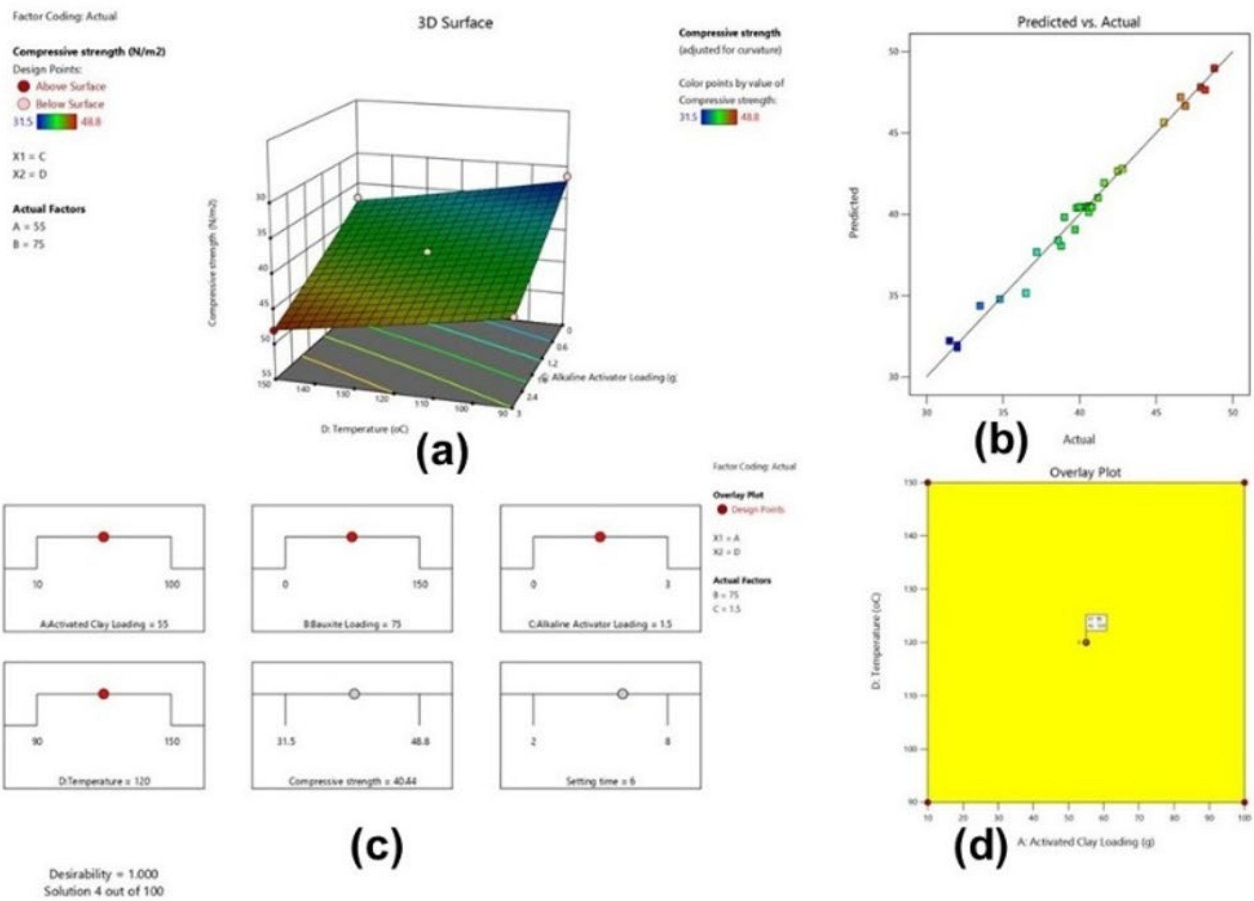

Figure 2. Optimization and validation of compressive strength using RSM.

studied range. Figure 3 (c) shows the 3D surface of activated clay loading (*A*) and alkaline activator loading (*C*) at constant bauxite content (75 g) and curing temperature (120 °C). Increasing alkaline activator loading significantly reduces setting time, reflecting accelerated dissolution and faster geopolymer gel formation. While higher activated clay content tends to increase setting time, its effect is moderated when sufficient activator is present. Figure 3 (d), the contour plot of activated clay loading (*A*) versus alkaline activator loading (*C*), further highlights that short setting times are achieved at higher activator dosages and lower clay contents. The diagonal contour pattern confirms the dominant role of alkaline activator loading in controlling setting kinetics [32-34]. The RSM analysis demonstrates that setting time is primarily controlled by alkaline activator loading, with activated clay and bauxite contents exerting secondary, retarding effects, while curing temperature (120 °C) provides a constant thermal environment that supports stable and predictable setting behavior. These findings support the optimization of setting time alongside compressive strength for practical oil-well cementing applications [35-37].

3.4. Analysis and Discussion of the Predicted vs. Actual Plot for Setting Time.

Figure 4 (a–d) presents the optimization and validation results for setting time using RSM. Figure 4 (a) shows the 3D response surface of bauxite loading (*B*) and curing temperature (*D*) at fixed activated clay loading (A = 55 g) and alkaline activator loading (C = 1.5 g). Setting time increases by increasing bauxite content and curing temperature, indicating that higher solid loading and thermal exposure tend to slow the setting process by moderating reaction kinetics and delaying structural buildup. Figure 4 (b) compares predicted and experimental setting time values. The close alignment of data points along the 45° line demonstrates excellent agreement between predicted and actual responses, confirming the adequacy and reliability of the developed model for setting time prediction [38-40]. Figure 4 (c) presents numerical optimization results based on the desirability function. The optimal conditions were identified as activated clay loading of 55 g, bauxite loading of 75 g, alkaline activator loading of 1.5 g, and curing temperature of 120 °C, yielding a predicted

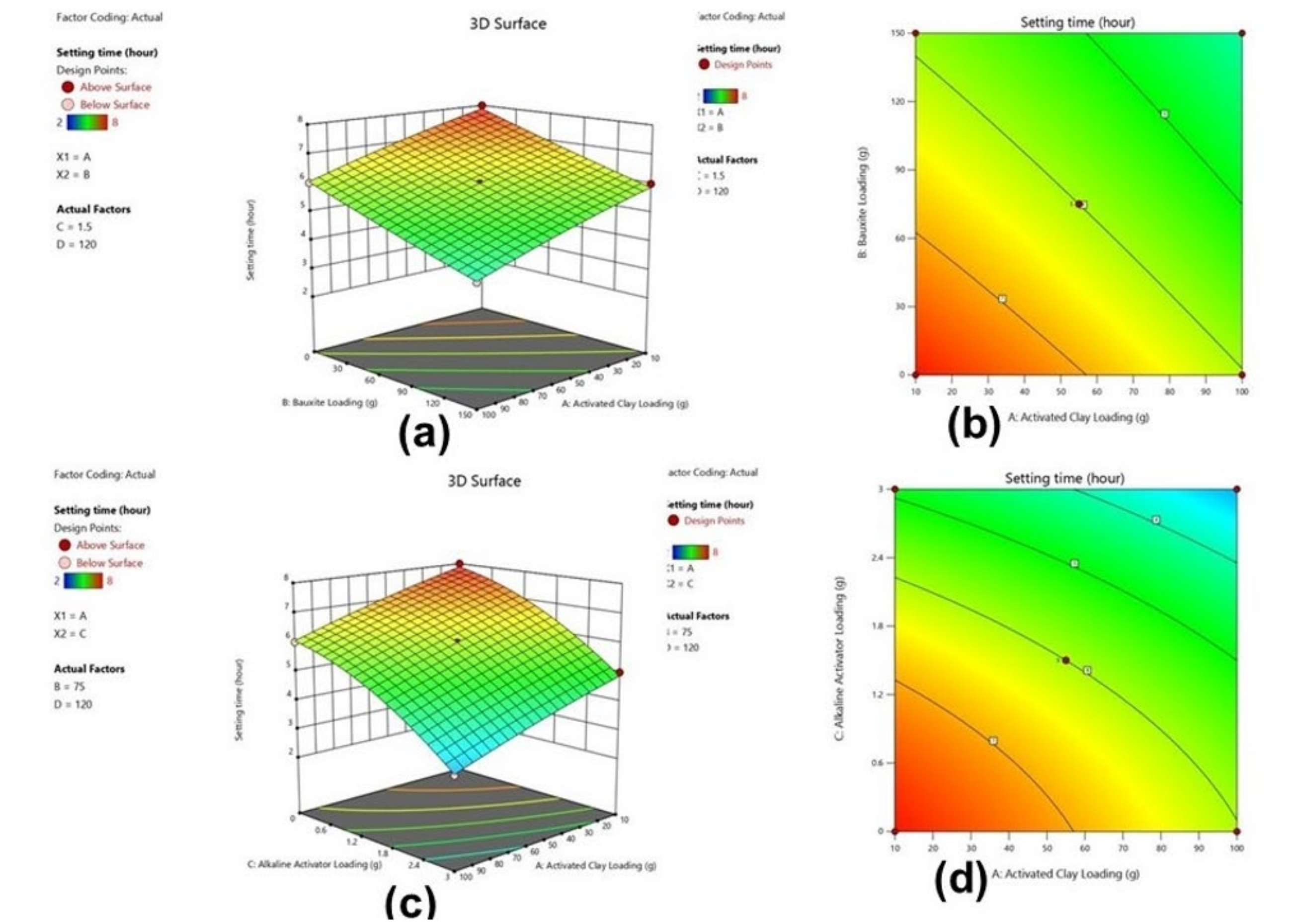

Figure 3. Response surface and contour plots illustrating the effects of activated clay, bauxite, alkaline activator, and curing temperature on optimizing setting time.

setting time of approximately 6 hours with a desirability value of 1.0. This confirms that the selected factor combination satisfies the target setting time requirement while maintaining acceptable compressive strength. Figure 4 (d) shows the overlay plot, where the highlighted region represents the feasible design space meeting the setting time criteria. The optimal point lies well within this region, indicating a stable and robust operating window [41-43]. Additionally, the results demonstrate that setting time is primarily influenced by bauxite loading and curing temperature, with activated clay and alkaline activator providing secondary control. The strong agreement between model predictions and experimental data validates the suitability of the optimized formulation for practical oil-well cementing applications [44-46]. Empirical mathematical model for setting time (Y_{st}, h) is as follow:

$$Y_{st} = +6.00 + 0.0833A + 0.5833B + 0.1667C + 0.0833D - 0.7500AB + 0.1250AC + 0.0000AD + 0.2500BC - 0.1250BD - 0.5000CD - 0.4167A^2 - 0.2917B^2 - 0.0417C^2 + 0.2083D^2 \quad (2)$$

4. Conclusions

This study successfully achieved the objectives of optimizing the setting time and compressive strength of a CBG binder for oil-well cementing applications using RSM. Firstly, the study systematically evaluated the effects of activated clay loading, bauxite loading, alkaline activator loading, and curing temperature on geopolymer performance. The results demonstrated that these variables interact significantly to control the geopolymerization process, with alkaline activator loading and curing temperature exerting the greatest influence on compressive strength and setting time. Secondly, reliable quadratic predictive models were successfully developed and statistically validated to describe the relationships between the processing variables and the response parameters. The close agreement between the predicted and experimental values confirmed the robustness and predictive capability of the developed models for geopolymer optimization. Third, numerical optimization using the desirability function identified the optimum formulation comprising 55

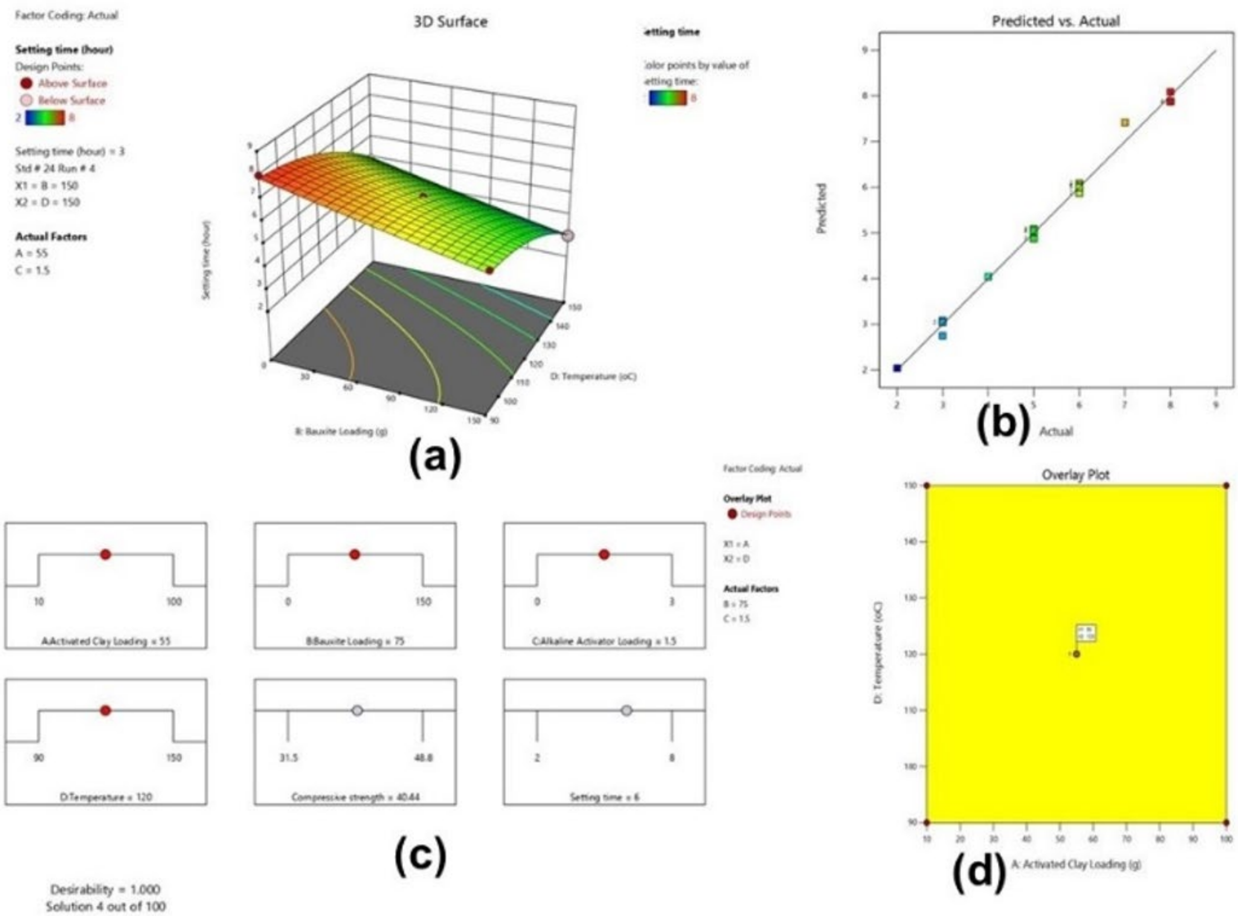

Figure 4. Optimization and validation of setting time using RSM.

g activated clay, 75 g bauxite, 1.5 g alkaline activator loading, and a curing temperature of 120 °C, yielding a compressive strength of approximately 40.4 MPa and a setting time of 6 h, demonstrating its suitability for oil-well cementing applications.

The scientific novelty of this work lies in the development of a clay–bauxite geopolymer binder specifically optimized for oil-well cementing through an integrated RSM-based optimization approach. Unlike previous studies that primarily investigated individual processing parameters or relied on conventional trial-and-error experimentation, this study establishes statistically validated predictive models that quantify the interactive effects of activated clay loading, bauxite loading, alkaline activator loading, and curing temperature on both fresh and hardened properties of the geopolymer binder. This provides new scientific knowledge on the optimization of clay-based geopolymer systems under conditions relevant to oil-well cementing.

This research advances the current state of knowledge by providing a systematic, statistically validated optimization framework for designing high-performance, low-carbon clay-based geopolymer binders capable of meeting the stringent performance requirements of oil-well cementing. The findings not only improve the understanding of the relationships between formulation variables and geopolymer performance but also provide a practical basis for the future development and industrial application of sustainable alternatives to conventional Ordinary Portland Cement in high-temperature and high-pressure well environments.

Acknowledgment

This research was financially supported by the Faculty of Chemical and Process Engineering Technology, Universiti Malaysia Pahang Al-Sultan Abdullah (UMPSA), through the UMP Fundamental Research Grant Scheme Grant Number (RDU220376). The authors extend their sincere gratitude for the funding and access to laboratory facilities, which were essential for the successful completion of the experimental work presented in this study.

CRedit Authors Statement

Author Contributions: Money Barima (MB): Writing original draft, Methodology, Investigation, Data curation, Formal analysis, Conceptualization of the study; Priyanga A/P Kailasanathan (PAK): Assisted in computational modeling and interpretation of results; Norasyikin Ismail (NI): Performed computational optimization; Abutu David (AD): Assisted in validation, project administration and interpretation of results; Siti Hajar Noor Shaarani (SHNS): Assisted in validation of the study; Norida Ridzuan (NR): Profound formal analysis; Siti Qurratu' Aini Mahat (SQAM). Provided critical revisions, funding acquisition, and technical insights. All authors have read and agreed to the published version of the manuscript.

References

[1] Hassan. S, Sivakumar, M. Alade, A.O. Ganesan, S. Miskam, M. (2025). Compressive strength of clay-based geopolymers: A concise review of the influencing factors and underlying mechanisms, *Appl. Clay Sci.*, 278, 107985. DOI: 10.1016/j.clay.2025.107985.

[2] Xu, W., Briffaut, M., Gay, N., Shao, J. (2025). Experimental investigation on the physical and mechanical properties of metakaolin-based geopolymers: Effects of aging and confining pressure, *Appl. Clay Sci.*, 276, 107910. DOI: 10.1016/j.clay.2025.107910.

[3] Ettahiri, Y. (2023). Comparative study of physicochemical properties of geopolymers prepared by four Moroccan natural clays, *Journal of Building Engineering*, 80, 108021. DOI: 10.1016/j.jobe.2023.108021.

[4] Barima, M., Siti, Q.A.B.M., Ismail, N. Rayan, H.M., Abutu, D., Agi, A.A. (2025). Clay-Based Geopolymers Cement for Oil Wells: A Bibliometric Analysis and Literature Review. Clay Science - Bridging Geology and Physical Chemistry, IntechOpen, 1-27. DOI: 10.5772/intechopen.1011806.

[5] Siyal, A.A., Hamidi, R.M., Shamsuddin, R.M.R., Mohamed, M.S.R., Ilyas, S.U. (2025). Optimization of flexural strength in fly ash-based geopolymers through response surface methodology, *Coatings*, 16 (4), 1706–1718. DOI: 10.1007/s43995-025-00205-1.

[6] Chen, W., Dong, B., Peng, K.-D., Yang, Q., Wang, Y., Hong, S. (2024). Optimization of microstructure and mechanical performance of clay-rich sand-washing slurry-based geopolymers, *Applied Clay Science*, 260, 107551. DOI: 10.1016/j.clay.2024.107551.

[7] Elataoui, K. (2024). Exploring the diversity of clays: Impacts of temperature on physicochemical changes, mechanical characteristics, and permeability, and their relevance to membrane applications, *Boletín de la Sociedad Española de Cerámica y Vidrio*, 63(6), 398–412. DOI: 10.1016/j.bsecv.2024.07.001.

[8] Barima, M. (2025). A review on advancing clay-based geopolymers for high-temperature oil well cements: Mechanisms, durability, and applications. *Petroleum Research*, 11(1), 274-296. DOI: 10.1016/j.ptlrs.2025.08.005.

[9] Singh, N.B., Kumar, M., Rai, S. (2020). Geopolymer cement and concrete: Properties, *Materials Today: Proceedings,* 29, 743–748. DOI: 10.1016/j.matpr.2020.04.513.

[10] Zamanian, M., Payan, M., Afsharnia, N. (2026). Thermo-mechanical behavior of clays: Divergent responses of kaolinite and montmorillonite in temperature-controlled shear tests, *Case Studies in Thermal Engineering*, 80, 107857. DOI: 10.1016/j.csite.2026.107857.

[11] Barima, M. (2025). Appraising the Impact of Activated Clay Geopolymer as a Sustainable Geopolymer Cement for Oilwell Applications. *SPE Nigeria Annual International Conference and Exhibition*, DOI: 10.2118/228642-MS.

[12] Almutairi, A.L., Tayeh, B.A., Adesina, A., Isleem, H.F., Zeyad, A.M. (2025). Potential applications of geopolymer concrete in construction: A review, *Case Studies in Construction Materials*, 15, e00733. DOI: 10.1016/j.cscm.2021.e00733.

[13] Khasawneh, M.A. (2025). Geopolymer concrete in construction projects: a review, *Discov. Civ. Eng.,* 2(1), 124. DOI: 10.1007/s44290-025-00281-1.

[14] Ikotun, J.O., Aderinto, G.E., Madirisha, M.M., Katte, V.Y. (2024). Geopolymer Cement in Pavement Applications: Bridging Sustainability and Performance, *Sustainability*, 16(13), 5417. DOI: 10.3390/su16135417.

[15] Wan, Q., Rao, F., Song, S., León-Patiño, C.A. (2017). Geothermal clay-based geopolymer binders: Synthesis and microstructural characterization, *Applied Clay Science*, 146, 23–229. DOI: 10.1016/j.clay.2017.05.047.

[16] Mostafa, N.Y., Mohsen, Q., El-maghraby, A. (2014). Characterization of low-purity clays for geopolymer binder formulation, *Int. J. Miner. Metall. Mater.,* 21(6), 609–619. DOI: 10.1007/s12613-014-0949-y.

[17] Sam-Tunsa, A.A., Epey, N., Nana, A., Tome, S., Mache, J.R., Nchare, M. (2022). Mineralogical and physicochemical characterization of clayey materials from Meiganga (Adamawa-Cameroon): potential application in traditional ceramic, *J. Build. Rehabil.*, 7(1), 65. DOI: 10.1007/s41024-022-00203-z.

[18] Adjei, S., Elkatatny, S., Aggrey, W.N., Abdelraouf, Y. (2022). Geopolymer as the future oil-well cement: A review, *Journal of Petroleum Science and Engineering*, 208, 109485. DOI: 10.1016/j.petrol.2021.109485.

[19] Migunthanna, J., Rajeev, P., Sanjayan, J. (2022). Waste Clay Bricks as a Geopolymer Binder for Pavement Construction, *Sustainability*, 14(11), 6456. DOI: 10.3390/su14116456.

[20] Buyondo, K.A., Olupot, P.W., Kirabira, J.B., Yusuf, A.A. (2020). Optimization of production parameters for rice husk ash-based geopolymer cement using response surface methodology, *Case Studies in Construction Materials*, 13, e00461, DOI: 10.1016/j.cscm.2020.e00461.

[21] Agrawal, A., Malviya, N. (2025). Advanced geopolymer concrete with coconut fiber reinforcement: optimizing strength, durability, and predictive modelling for sustainable construction, *Archit. Struct. Constr.*, 5(1), 39. DOI: 10.1007/s44150-025-00152-4.

[22] Tome, S. (2022). Structural and Physico-mechanical Investigations of Mine Tailing-Calcined Kaolinite Based Phosphate Geopolymer Binder, *Silicon*, 14(7), 3563–3570. DOI: 10.1007/s12633-021-01137-w.

[23] Mahmoodi, O., Siad, H., Lachemi, M., Dadsetan, S., Sahmaran, M. (2020). Optimization of brick waste-based geopolymer binders at ambient temperature and pre-targeted chemical parameters, *Journal of Cleaner Production*, 268, 122285. DOI: 10.1016/j.jclepro.2020.122285.

[24] Kumari, N., Mohan, C., Negi, A. (2023). An Investigative Study on the Structural, Thermal and Mechanical Properties of Clay-Based PVC Polymer Composite Films, *Polymers*, 15(8), 1922. DOI: 10.3390/polym15081922.

[25] Barima, M. (2025). Characterization of Kuala Rompin clay (KRC) and empty fruit bunch ash (EFBA) for potential application in the formulation of geopolymer cement, *Discov. Concr. Cem.*, 1(1), 12. DOI: 10.1007/s44416-025-00012-w.

[26] Kaze, C.R. (2022). Thermal behaviour and microstructural evolution of metakaolin and meta-halloysite-based geopolymer binders: a comparative study, *J. Therm. Anal. Calorim.*, 147(3), 2055–2071. DOI: 10.1007/s10973-021-10555-2.

[27] Yin, R., Zhu, L., Cheng, D., Liang, P., Gao, R. (2026). Multi-Objective Optimization Design of a Metakaolin–Slag-Based Binary Solid Waste Geopolymer Mortar Mix Proportion Using Response Surface Methodology, *Buildings*, 16(2), 402. DOI: 10.3390/buildings16020402.

[28] Quiatchon, P.R.J. (2021). Investigation on the Compressive Strength and Time of Setting of Low-Calcium Fly Ash Geopolymer Paste Using Response Surface Methodology, *Polymers*, 13(20), 3461. DOI: 10.3390/polym13203461.

[29] Lekshmi, S., Sudhakumar, J. (2022). An assessment on the durability performance of fly ash-clay based geopolymer mortar containing clay enhanced with lime and GGBS, *Cleaner Materials*, 5, 100129. DOI: 10.1016/j.clema.2022.100129.

[30] Neufville, E.K., Kanali, C., Mogire, P. (2024). Assessing the Mechanical and Micro-Structural Properties of Concrete with Silica Fume and Coconut Shell as Partial Replacements of Cement and Fine Aggregates, *International Journal of Civil Engineering*, 11(4), 39–53. DOI: 10.14445/23488352/IJCE-V11I4P105.

[31] Khalid, L.W., Mermerdaş, K., Ekmen, Ş., Khidhir Bzeni, D. (2026). Optimization of fresh and hardened properties of fiber-reinforced 3D printed geopolymer composites using response surface Methodology: A data-driven approach based on prior experimental studies, *Journal of Building Engineering*, 117, 114655. DOI: 10.1016/j.jobe.2025.114655.

[32] David. A. (2025). Reinforcing concrete with nano-enhanced bio-additives: a path toward sustainable construction materials, *Discov. Concr. Cem.*, 1(1), 20. DOI: 10.1007/s44416-025-00022-8.

[33] Abolhasani, A., Samali, B., Dehestani, M., Libre, N.A. (2022). Effect of rice husk ash on mechanical properties, fracture energy, brittleness and aging of calcium aluminate cement concrete, *Structures*, 36, 140–152. DOI: 10.1016/j.istruc.2021.11.054.

[34] Wang, W.Lv.B., Zhang, C., Li, N., Pu, S. (2023). Mechanical and micro-structure characteristics of cement-treated expansive soil admixed with nano-MgO, *Bull. Eng. Geol. Environ.*, 82(2), 48. DOI: 10.1007/s10064-022-03055-6.

[35] Kamali, M., Khalifeh, M., Saasen, A., Godøy, R., Delabroy, L. (2021). Alternative setting materials for primary cementing and zonal isolation – Laboratory evaluation of rheological and mechanical properties, *Journal of Petroleum Science and Engineering*, 201, 108455. DOI: 10.1016/j.petrol.2021.108455.

[36] Armah, E.A., Koffi, H.A., Amuzu, J.K.A. (2020). Compressive and Flexural Strengths of Concrete Containing Ground Palm Kernel Shells as Partial Replacement of Cement, *Journal of Modern Materials*, 7(1), 7–16. DOI: 10.21467/jmm.7.1.7-16.

[37] Bayuaji, R. Kurniawan, R. W. Yasin, A. K. Fatoni, H. A. Lutfi, F. M. A. (2016). The effect of fly ash and coconut fibre ash as cement replacement materials on cement paste strength, *IOP Conf. Ser.: Mater. Sci. Eng.*, 128, 012014. DOI: 10.1088/1757-899X/128/1/012014.

[38] Edeh, J.C., Peters, J.F., Eni-Ikeh, S.N., Abuh, M.A., Ndubisi, P.C. (2024). Reinforcement of cement tiles with palm kernel shell particles as natural fibre, *Nigerian Journal of Technology*, 43(1), 64–70. DOI: 10.4314/njt.v43i1.9.

[39] Wang, W. (2021). Influence of Carbonization Process on the Mechanical Properties of Nano-MgO Modified Cement Soil, *Sustainability*, 13(6), 3558. DOI: 10.3390/su13063558.

[40] Nwaichi, P.I., Ridzuan, N., Nwaichi, E.O., Umunnawuike, C., Abutu, D., Nyah, F., Money, B., Agi, A. (2025). Advances in oilwell cement retarders: a bibliometric and systematic review of mechanisms, challenges, emerging trends, and future directions. *Discover Concrete and Cement*, 1(1), 8. https://doi.org/10.1007/s44416-025-00008-6.

[41] Lumbab, J.S., Bongo, J., Moralde, R.M., Villaceran, G.I. (2023). Coconut Shell Ash as Partial Substitute to Cement in Concrete Hollow Blocks, *IOP Conf. Ser.: Earth Environ. Sci.*, 1184(1), 012024, DOI: 10.1088/1755-1315/1184/1/012024.

[42] Money, B., Shaarani, S.H.N., Modather, R.H., Abutu, D., Mahat, S.Q. (2026). Clay-based geopolymer cement with industrial additives for improved rheological thermal and microstructural performance. *Discov. Concr. Cem.* 2(1), 29. DOI: 10.1007/s44416-026-00071-7

[43] Mahat, S.Q.A., Nwaichi, P.I., Umunnawuike, C., Nyah, F., Abutu, D., Money, B., Gbonhinbor, J.R., Nwaichi, E.O., Agi, A. (2025). Optimizing Drilling Fluid Performance with Green Inhibitors. *SPE Nigeria Annual International Conference and Exhibition.* DOI: 10.2118/228648-MS

[44] Al_Ani, M., Sidek, M.A., Jaafar, M.Z., Gbonhinbor, J.R., Abutu, D., Money, B., Agi, A. (2025). Synthesis, Characterization and Oil Recovery Mechanisms of a Novel Polymeric Nanofluid for High Temperature and High salinity Oil Reservoirs. *SPE Nigeria Annual International Conference and Exhibition.* DOI: 10.2118/228636-MS

[45] Money, B., Mahat, S.Q.A.B., Ismail, N., Aziz, M.A.B.A., Randy, G.J., Modather, R.H., Umunnawuike, C., Nwaichi, P.I., Nyah, F., David, A., Agi, A. (2025). A Comprehensive Approach to Health, Safety, and Environmental Sustainability in Drilling: Balancing Operational Efficiency with Safety Standards. *SPE Nigeria Annual International Conference and Exhibition*, DOI: 10.2118/228635-MS

[46] Nyah, F., Ridzuan, N., Epelle, E., Bin Abd Aziz, M.A., Money, B., Abutu, D., Agi, A. (2025). Cellulose Bionanomaterial Design for Enhanced Oil Recovery: A Review of Existing, Emerging Technologies and Future Outlook. *Petroleum Research*, 11(2), 641-686. DOI: 10.1016/j.ptlrs.2025.12.002.